Continuous wave sonar with hyperbolic frequency modulation keyed by pseudo-random sequence

Andrzej JEDEL, Jacek MARSZAL, Roman SALAMON

Gdansk University of Technology
Faculty of Electronics, Telecommunications and Informatics
G. Narutowicza 11/12, 80-233 Gdansk, Poland
andrzej.jedel@eti.pg.gda.pl

A CW FM type sounding signal is used in the classical solution of silent sonar. While the signal provides a relatively simple implementation of digital signal processing, and ensures good detection conditions, unfortunately, in the presence of the Doppler effect, distance measurement results tend to be wrong. This is due to the fact that the received signal's instantaneous frequency value is dependent both on the distance to the object, and its speed. Sounding signal, as patented by the authors, is a combination of Pseudo-Random Sequences (PRS), and elementary signals of Hyperbolic Frequency Modulation (HFM) type. The structure of this signal is aimed at minimizing measurement error. The article presents the idea of a sounding signal of HFM+PRS type, and the results of computer simulations.

Keywords: CW FM, pseudorandom sequence, Doppler effect, matched filtering.

1. Introduction

In use for several decades, continuous wave (CW) and linear frequency modulation (FM) sonars are low power, short range, and easy to handle devices for divers. There have been attempts in recent years to redesign CW FM sonars to serve other purposes, such as silent sonar, that are not easily detected by intercept sonars [4, 5, 7, 8, 9, 10, 13, 14] and Continuous Active Sonars (CAS) for continuous observation of remote moving targets [2, 3, 15, 17].

Because silent sonar uses continuous periodical signals with linear or hyperbolic frequency modulation coupled with correlational reception of echo signals, the power of its sounding signal is lower than that of conventional pulse sonars, but the ranges and resolutions remain the same [4, 8, 9, 13]. Pulse sonars measure target location over a period which is equal to the period of sounding signal emission. In the case of long-range sonars, it can be equal even to one minute. For a fast moving target, this is long enough to change its position

significantly, which is clearly a problem, especially for military sonars. In CW FM sonars, a change in target location is recorded as a change in instantaneous frequency of the echo signal which can be used for continuous target tracking.

The downside of CW FM sonars using frequency to determine the location of moving targets, is that they misread the distances as a result of the Doppler effect [1, 5, 6, 7, 9, 11]. The error in this case is usually bigger than that in pulse sonars, to the extent of becoming unacceptable at times. To reduce the error, continuous binary pseudorandom sequences are proposed, with switching of two different short-term signals whose frequency changes over time. The article presents a modified and more detailed version of a previous solution [12]. The results of simulation tests are given, presenting how moving target distances are misread. A comparison to the errors of the basic and simple version of the CW FM sonar is made.

2. Distance measurement errors in CW FM sonar

Let us consider the operation of a CW FM sonar in the basic version emitting periodical signals with hyperbolic frequency modulation (HFM). The sonar's capacity for detecting echo signals off moving targets is better than that of a sonar using linear frequency modulation (LFM) [5, 6, 7, 16]. A single period T of an HFM signal with frequency increasing over time is described with the following formula:

$$s^{+}(t) = s_o \cdot \sin[-2\pi \cdot \frac{T \cdot f_l \cdot f_h}{B} \cdot ln\left(1 - B \cdot \frac{t}{T \cdot f_h}\right)] \quad t \in (0, T), \tag{1}$$

where f_l, f_h are the upper and lower spectrum frequencies accordingly, and $B = f_h - f_l$ is spectrum width.

An HFM signal with frequency decreasing over time takes this form:

$$s^{-}(t) = s_o \cdot \sin[2\pi \cdot \frac{T \cdot f_l \cdot f_h}{B} \cdot ln\left(1 + B \cdot \frac{t}{T \cdot f_l}\right)] \quad t \in (0, T). \tag{2}$$

Instantaneous frequency is a derivative of signal phase, and in the case of signal $s^{+}(t)$ amounts to:

$$f^{+}(t) = \frac{f_l}{1 - B \cdot \frac{t}{T \cdot f_h}} \qquad t \in (0, T), \tag{3}$$

and in the case of signal $s^{-}(t)$:

$$f^{-}(t) = \frac{f_h}{1 + B \cdot \frac{t}{T \cdot f_l}} \qquad t \in (0, T). \tag{4}$$

As we can see from formula (3) $f^{+}(0) = f_l$ and $f^{+}(T) = f_h$, and so frequency increases over time. By analogy, from formula (4) we have $f^{-}(0) = f_h$ and $f^{-}(T) = f_l$, which means that signal frequency decreases over time.

Sounding signal described with formula (1) or formula (2) is reflected from a target moving towards the sonar with velocity v. The echo signal from a target which is away from the sonar by R_0 at a moment of time $t = 0$, is received after time $\tau = 2R_0/(c+v)$, where c is the velocity of acoustic wave propagation in water. As the target is moving, the Doppler effect causes time compression at compression rate of $d = (c+v)/(c-v)$. As a result, the echo signal duration is shorter (for $v < 0$ – longer) and amounts to T/d. Echo signals can thus be written down as:

$$x^{+}(t) = x_o \cdot \sin[-2\pi \cdot \frac{T \cdot f_l \cdot f_h}{B} \cdot ln\left(1 - B \cdot \frac{d \cdot (t - \tau)}{T \cdot f_h}\right)] \qquad t \in (0, T/d), \tag{5}$$

and

$$x^{-}(t) = s_o \cdot \sin[2\pi \cdot \frac{T \cdot f_l \cdot f_h}{B} \cdot ln\left(1 + B \cdot \frac{d \cdot (t-\tau)}{T \cdot f_l}\right)] \qquad t \in (0,\ T/d)\ . \qquad (6)$$

As a consequence, instantaneous frequencies of echo signal are expressed with the following relations:

$$f^{+}(t) = \frac{d \cdot f_l}{1 - B \cdot \frac{d \cdot (t-\tau)}{T \cdot f_h}} \qquad t \in (\tau,\ \tau + T/d)\ , \qquad (7)$$

and

$$f^{-}(t) = \frac{d \cdot f_h}{1 + B \cdot \frac{d \cdot (t-\tau)}{T \cdot f_l}} \qquad t \in (\tau,\ \tau + T/d)\ . \qquad (8)$$

From formula (7) which describes frequency increasing over time, we have: $f^{+}(\tau) = d \cdot f_l$, and $f^{+}(\tau + T/d) = d \cdot f_h$. From formula (8) which describes frequency decreasing over time, we obtain: $f^{-}(\tau) = d \cdot f_h$, a $f^{-}(\tau + T/d) = d \cdot f_l$. As you can see, in both cases there is a shift in the cut-off frequencies of echo signal spectrum; they went up when $v > 0$ ($d > 1$) and went down when $v < 0$ ($d < 1$). Spectrum width has changed to reach $d \cdot B$.

To reduce the number of digital operations in the sonar's receiver, quadrature sampling is used. The frequency of quadrature sampling is $f_s = f_0/k$, where k is a natural number and depends on signal spectrum width. The samples are treated as real and imaginary components of complex samples and create a complex, low-pass form of echo signal. The sounding signal is sampled in the same way. Figure 1 shows the module of a sounding signal spectrum $|S_q(f)|$ and the module of echo signal spectrum $|X_q(f)|$ after quadrature detection.

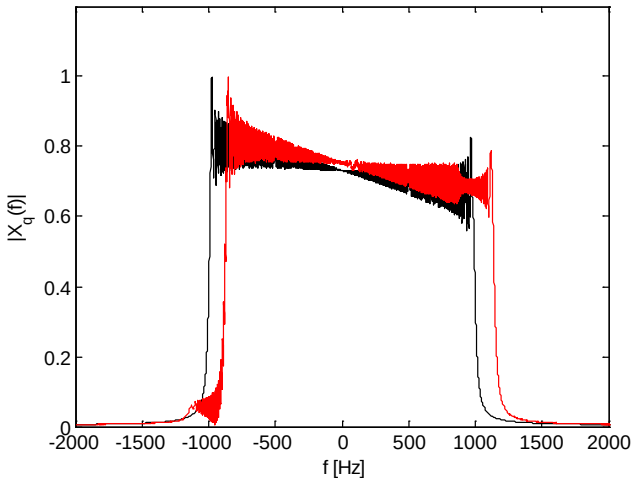

Fig. 1. Spectrum of the sounding signal (black) and echo signal (red) (f_0 = 10 kHz, B = 2 kHz, T = 2 s, $f_s = f_0/2$, v = 10 m/s, c = 1500 m/s).

The correlation function between the digital sounding signal after quadrature detection marked as $s_q(n)$, and the complex periodical echo signal $x_q(n)$ is calculated in the receiver. The period of the function is $N_0 = f_s \cdot T/d$, within which the signal is the result of continuous signal quadrature sampling as described in formulas (4) or (5). The output signal takes this form:

$$y(m) = \sum_{n=0}^{N-1} s_q^{*}(n) \cdot x_q(n+m)\ . \qquad (9)$$

Figure 2 shows the calculation result of the correlation function module at a point when the target was R_0 = 800 m away, moving towards the sonar at a speed of v = 10 m/s when the first sounding pulse was sent. The other sonar parameters are given in the caption to Figure 1. The red line shows the actual distance to the target when the echo signal is received in the particular measurement cycle. As the frequency of the sounding signal increases over time, the output echo signals are to the left of the line, and to the right as the frequency decreases. Figure 3 shows signals that are analogous to those in the previous Figure for target speed v = 5 m/s.

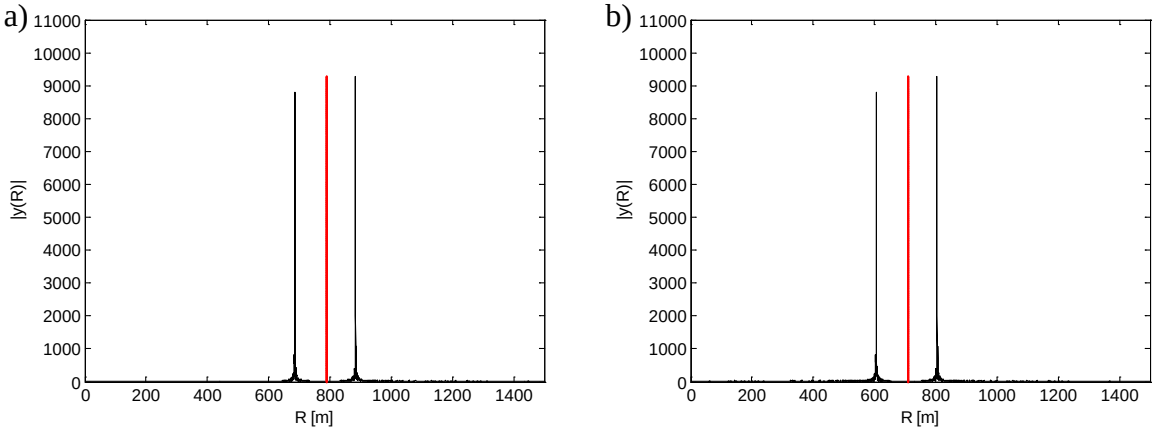

Fig. 2. Output signals (v = 10 m/s): a) – first measurement cycle, b) – fifth measurement cycle.

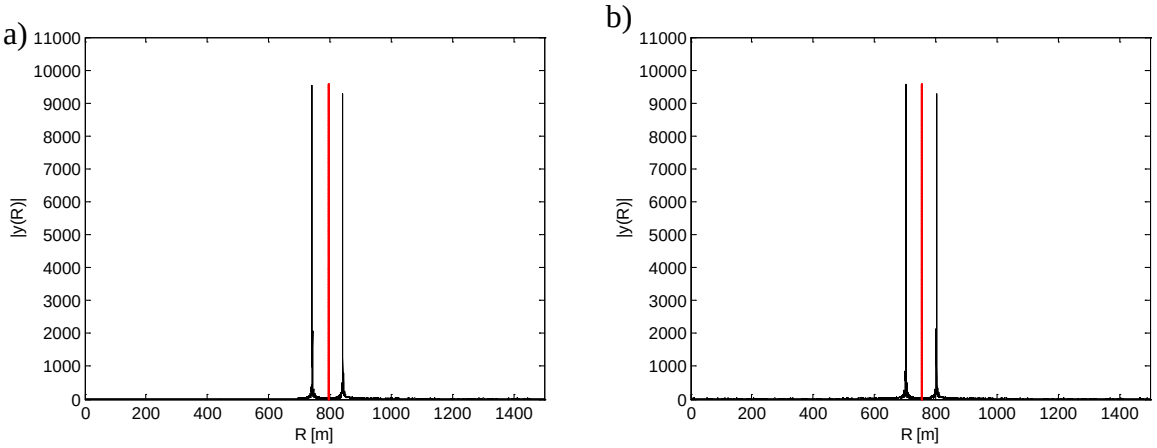

Fig. 3. Output signals (v = 5 m/s): a) - first measurement cycle, b) - fifth measurement cycle.

The Figures above illustrate the important features of the sonar, namely:

- very good distance resolution; output signal duration is inversely proportional to spectrum width B, and does not depend on time T,
- there is almost no relation between the height of HFM signal correlation maxima and target velocity v, which is an advantage over the LFM signal,
- the distance to target measurement error increases as target speed increases, and has no relation to the distance between target and sonar,
- the error sign depends on the direction of frequency change (ascending or descending over time).

Theoretical analysis and the measurements have shown that the distance measurement error ΔR can be described with the following approximate formula [5, 6]:

$$\Delta R \cong -v \cdot T \cdot \left(\frac{f_0}{B}\right). \tag{10}$$

The accuracy of error estimation using the above formula is not worse than ±10%.

Formula (10) applies to signals whose frequency increases over time. When measuring the distance to the target as it moves towards the receiver, the actual distance is underestimated. As it moves away from the receiver ($v < 0$), the result is an overestimation of the distance. For a frequency decreasing over time, distance measurement errors are just the opposite, as shown in Figure 2 and Figure 3.

For high target speeds and long duration T, which is necessary to ensure a long range ($R_{max} < c \cdot T/2$) and reduce the power of the signals, the measurement errors become unacceptable. As an example, for $v = 10$ m/s, $T = 10$ s and $f_0/B = 5$, the error is $\Delta R \cong 500$ m. The next chapter presents a method for reducing the error in measuring the distance to a moving target.

3. Method for reducing error in measuring the distance to moving targets

The objective is to identify a method for sounding signal modulation and detection which will combine the advantages of a short sounding pulse offering a fairly accurate distance measurement, and those of a continuous sounding signal with lower power and continuous target tracking. The main idea of the solution is directly related to the above assumptions, and involves a combination of elementary short duration signals (to ensure that distance measurement errors are minimised) with a pseudorandom sequence with narrow autocorrelation functions (to produce a continuous sounding signal). The elementary signals in this case are HFM signals offering good detection capability. The pseudorandom sequence (PRS), for example, will be represented by periodical maximum length sequences (MLS) with a selected order N. Figure 4 shows three periods of a sequence of the order N in the form of a signal $s_M(t)$. The number of elements in a single sequence is $M = 2^N - 1$. The correlation function $r_{ss}(t)$ between this signal and a single sequence period $s_1(t)$ is given in Figure 5. The time elapsed between the adjacent elements of the sequence equal to the duration of elementary signals, amounts to T_e , while the period of a single sequence is $T_s = M \cdot T_e$.

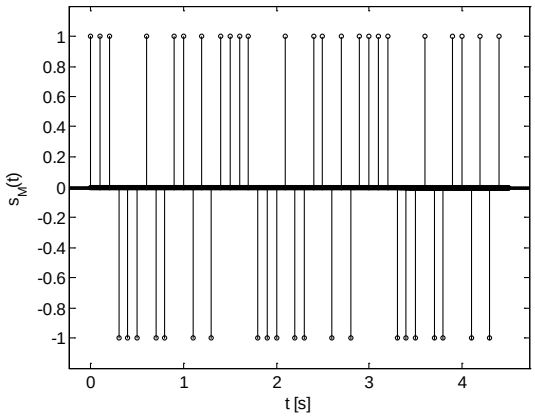

Fig. 4. Three MLS sequences ($M = 15$, $T_e = 0.1$ s).

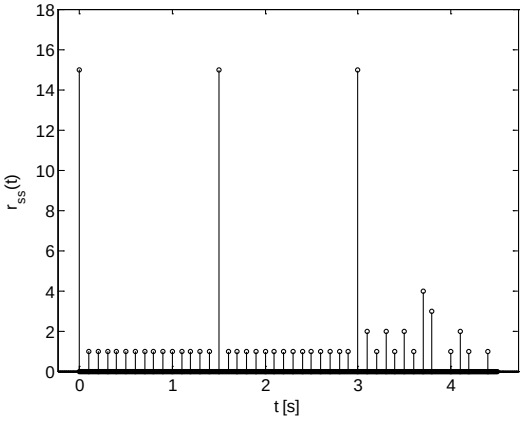

Fig. 5. Correlation function between three MLS sequences and a single sequence period.

The correlation function $r_{ss}(t)$ has its maximum value at $r_{ss}(0) = M$ with the side lobe level equal to 1, irrespective of the order N of the sequences. Elements of the MLS sequence are represented by elementary HFM signals: the positive ones represented by signal $s^+(t)$ with

a lower centre frequency f_0^+, and the negative ones by signal $s^-(t)$ with a higher centre frequency f_0^-. Because frequency changes in both elementary signals follow opposite directions, and the signs of elementary errors are different (Figure 2, Figure 3), the directions compensate each other which improves measurement accuracy. The width of the spectrum of both signals B_e is a fraction of half the width of spectrum B. This ensures that elementary signals are sufficiently separated. Signals $s^+(t)$ and $s^-(t)$ undergo quadrature sampling which produces low-pass signals $s_q^+(t)$ and $s_q^-(t)$. The signals are used in the receiver for echo signal correlation. Examples of normalised amplitude spectra $|S_q^+(f)|$ and $|S_q^-(f)|$ of elementary HFM signals after quadrature sampling are given in Figure 6 .

The signal is emitted by the sonar's transmitting array, and when it is reflected from a moving target it is picked up by the receiving array. The received echo signal $x(t)$ is delayed relative to the successive sequences of the transmitted signal and is compressed over time as a result of the Doppler effect. This causes the spectrum to shift and deform. The spectrum of echo signal after quadrature sampling is shown in Figure 7.

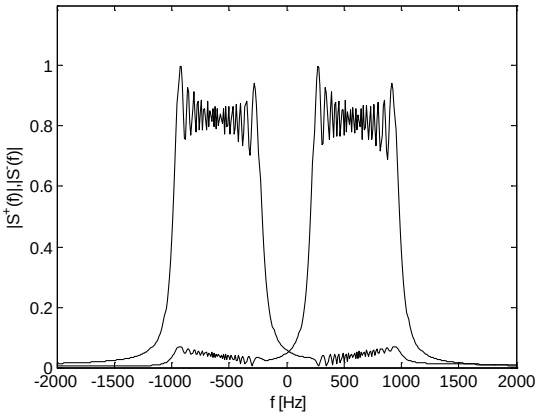

Fig. 6. Amplitude spectrum of transmitted signal ($f_{0q}^+ = -600$ Hz, $f_{0q}^+ = 600$ Hz, $B_e = 800$ Hz, $T_e = 0.1$ s).

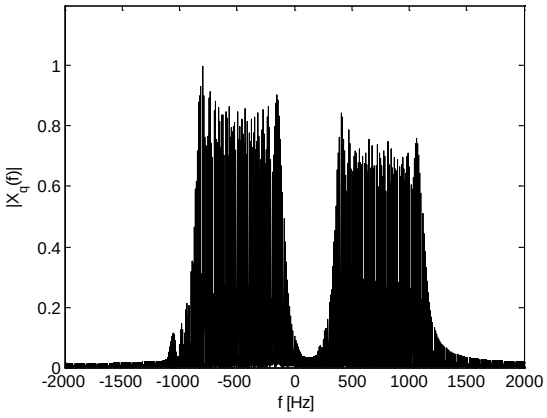

Fig. 7. Amplitude spectrum of echo signal (v = 10 m/s).

Echo signal operations are performed in the receiver. Figure 8 shows its functional diagram. The input echo signal $x(t)$ undergoes quadrature sampling, and analogue to digital conversion, as a result of which we obtain $x_q(n)$.

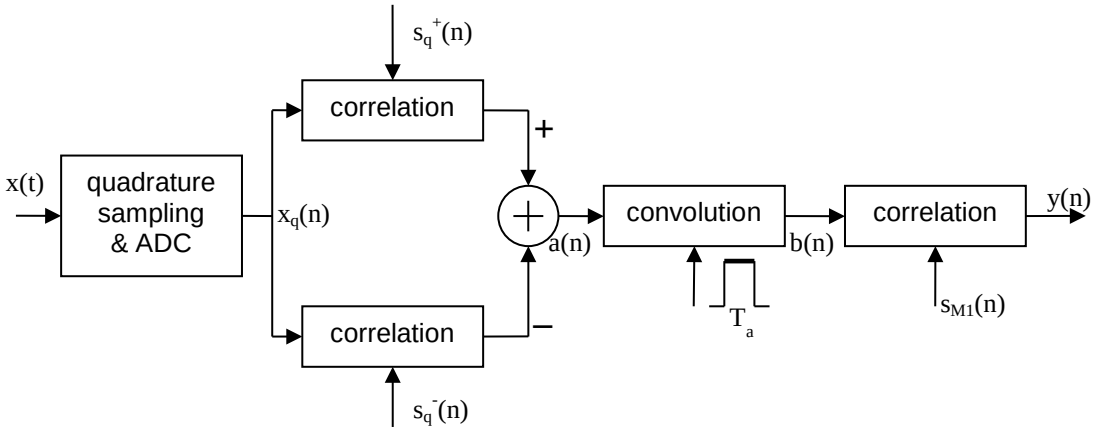

Fig. 8. Functional diagram of the receiver.

Next, correlation functions are calculated between signal $x_q(n)$ and elementary HFM signals $s_q^+(n)$ and $s_q^-(n)$. For echoes off a fixed target, the signals are fully correlated with the relevant transmitted signals. The successive correlation function maxima are proportional to the energy of echo signals, and their durations are inverse to spectrum width B_e. The entire sequence of the signals received is delayed relative to the transmitted signal only by $\tau = 2 \cdot R_0/c$, where R_0 is the target to sonar distance, and c is the velocity of the acoustic wave in water.

Because the complex values of correlated signals produce positive maximums of the correlation function, if the MLS sequence is to be reproduced, the signals after correlation are subtracted. The resulting signal is shown in Figure 9.

If the target moves at velocity v towards the sonar, the delay of the first element of the measurement cycle is $\tau = 2 \cdot R_0/(c+v)$, while the other signals are compressed over time. The effect of compression is that the duration of each received sequence is T_s/d, and the duration of a received single elementary HFM signal is T_e/d. As an example, the MLS sequence in Figure 9 contains $M = 15$ elements, the distance to target when the measurement cycle starts is $R_0 = 300$ m, ($\tau = 0.4$ *s)* and the target is moving towards the sonar at $v = 5$ m/s. The parameters of elementary HFM signals are given in the caption to Figure 6.

As a result of the Doppler effect, received elementary HFM signals after correlation shift over time. Its duration results from the formula (10) and amounts to:

$$\Delta t \cong \pm 2 \cdot T_e \cdot \frac{v}{c} \cdot \frac{f_0}{B_e} \ , \tag{11}$$

where the minus sign refers to elementary signals with an increasing frequency, and the plus sign refers to elementary signals with a decreasing frequency. Because the number of positive and negative elements in an MLS sequence always differs by one, the total error related to HFM signals is described with formula (11).

With the compression of received signals duration, and the shift in time of HFM correlation function maxima, a direct correlation between an MLS sequence, as shown in Figure 4, and signal $a(n)$ from Figure 9, produces a completely unsatisfactory result. This is illustrated in Figure 10. To eliminate the effect, the moving signal average $a(n)$ is determined by convoluting signal $a(n)$ with the averaging rectangular pulse whose duration of moving averaging is $T_a = p \cdot T_e$, where $0 > p > 1$ is the averaging coefficient. Figure 11 shows the result $b(t)$ of the operation for signal $a(t)$ from Figure 9 and for the rectangular pulse whose duration is $T_a = 0.2\ T_e$.

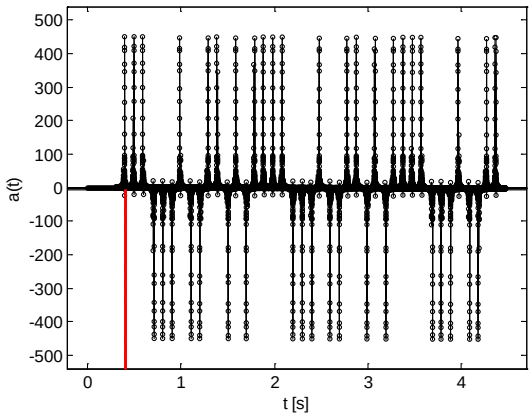

Fig. 9. Echo signal after correlation with elementary HFM signals.

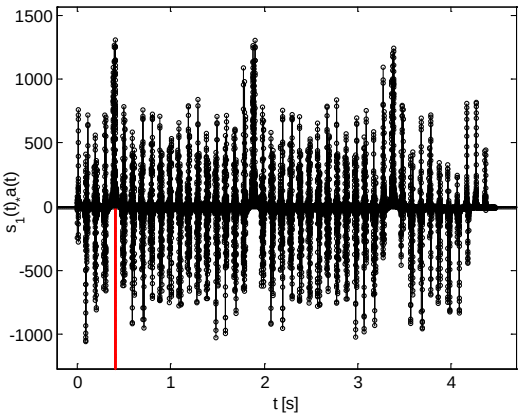

Fig. 10. Result of signal correlation: $s_1(t)$ and a(t).

The final result of signal processing in the sonar's receiver is obtained by calculating the correlation function between signal $b(n)$ and a single MLS sequence $s_{M1}(n)$, where the individual lines (shown in Figure 4) are replaced with rectangular pulses whose duration is T_a. Figure 12 shows the MLS sequences after the modification.

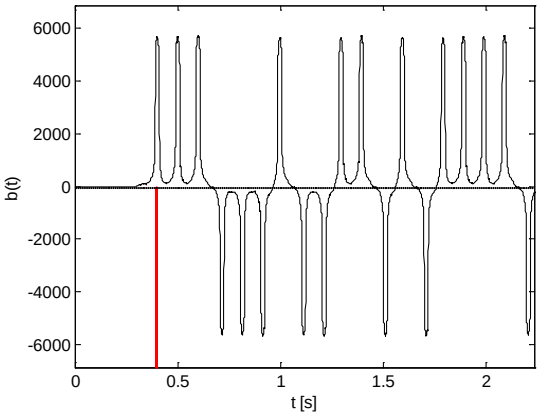

Fig. 11. Result of convolution of signal $a(t)$ with averaging rectangular pulse.

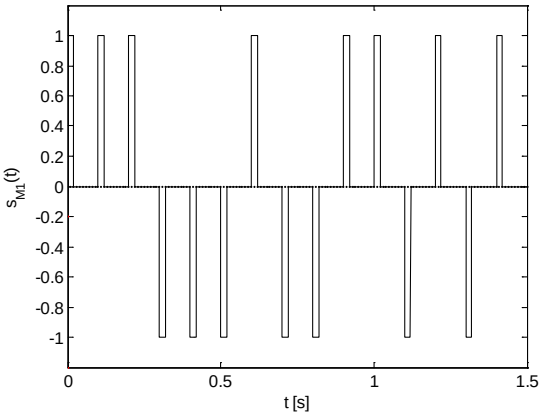

Fig. 12. Modified MLS sequence.

Figure 13 and Figure 14 show the signals after correlation. The chart in Figure 13 presents the output signal in the distance function in the first cycle of MLS sequence. Figure 14, on the other hand, shows the output signal from cycle two. The red line shows the actual distance to target at the moment when the received echo reaches its maximum. The difference between the actual distance, and the distance which matches the output signal's maximum, is the measurement error ΔR. The error, as exemplified in Figure 13 and Figure 14, amounts to –3.3 m and 2.6 m respectively. In an analogous basic version of sonar, the distance measurement error determined from formula 10 is approximately equal to –37 m, i.e. more than ten times bigger. The maximum level of side lobes depends on the order of the MLS sequence, and amounts to –30 dB, with distance resolution (set at –3 dB relative to the signal's maximum) equal to 19.8 m. Performed prior to correlation, moving averaging has deteriorated the resolution. It has, however, radically reduced the target distance measurement error, and eliminated clutter, the result of the mismatch caused by the Doppler effect.

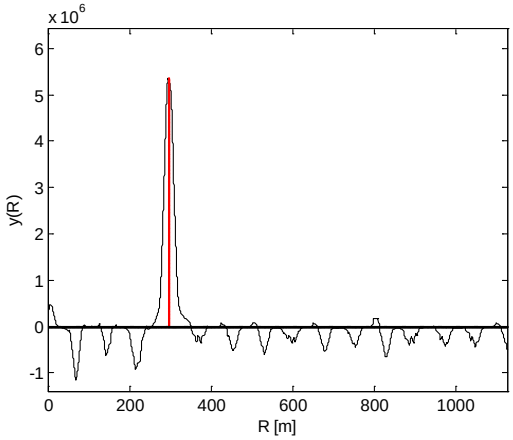

Fig. 13. Output signal in the first cycle. MLS (f_o = 10 kHz, B = 2 kHz, B_e = 0.4 kHz, T_s = 0.1 s, p = 0.2, M = 15, v = 10 m/s).

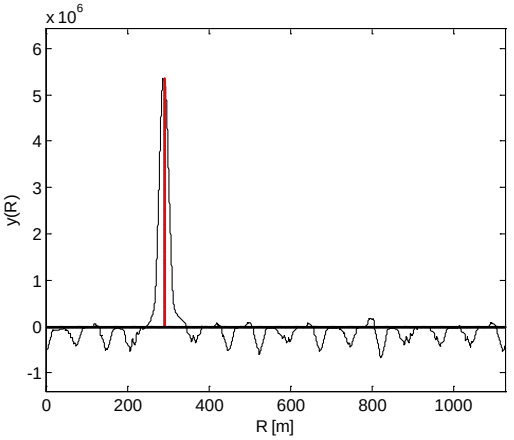

Fig. 14. Output signal in the second MLS cycle (parameters as in Figure 13).

4. Sonar parameters

The suggested solution is systemic in character, and allows for a wide selection of basic operating sonar parameters such as: range, anticipated maximum target speed, resolution and error in measuring the distance to the target, level of side lobes and the signal to noise ratio SNR_o. The parameters depend on the order N of *MLS* sequence, duration of elementary signals T_e and the averaging coefficient p. A change in any of the parameters results in changes in several other system parameters, and the outcomes may be positive or negative. The design will clearly require some optimisation. Some concessions will have to be made as well. For the purposes of this paper we are only going to present the basic relations between N, T_e and p and the sonar's operating parameters.

The range R_{max} of the sonar is limited by the relation:

$$R_{max} = 0.5 \cdot c \cdot M \cdot T_e = 0.5 \cdot c \cdot (2^N - 1) \cdot T_e \cong c \cdot 2^{N-1} \cdot T_e \,. \tag{12}$$

The desired range can be achieved for different combinations of the order N of MLS sequence and time T_e. Higher orders N of MLS sequences and shorter times T_e tend to produce better results. This regularity is presented in Figure 15. For an order of sequences $N = 5$ the distance measurement error is $\Delta R = -1$ m with distance resolution at 19 m. For an order of sequences $N = 4$ and double the time T_e, the distance measurement error goes up to $\Delta R = -8$ m, with distance resolution up to 37 m. In both cases the maximum level of side lobes is -27 dB, although for a higher order of sequences, the increase in the number and average level of lobes is quite significant. Excessive reductions in elementary signal duration T_e and the value of the averaging coefficient p cause the output signal pulse to split, which is unacceptable.

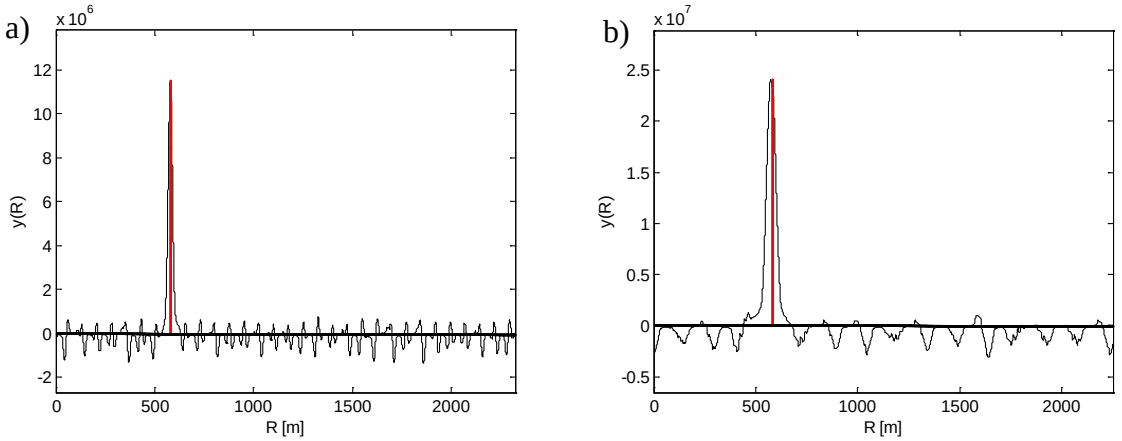

Fig. 15. The effect of selecting the order N of MLS sequences and duration T_e: a) $N = 5$, $T_e = 0.1$ s, b) $N = 4$, $T_e = 0.2$ s. ($f_0 = 10$ kHz, $B = 2$ kHz, $B_e = 0.4$ kHz, $p = 0.2$, $v = 5$ m/s).

The distance measurement error ΔR increases along with target speed v, and depends on how well the order of sequence N, time T_e and coefficient p are selected. In general, increasing the order of sequence N, and decreasing values T_e and p (only as far as reasonable) reduces the distance measurement error, as can be seen in Figure15. In both cases shown in the Figure, the error could be significantly reduced compared to the basic sonar result, which was $\Delta R = 75$ m.

Increasing the *maximum foreseeable target speed* has a negative effect on the distance measurement error, distance resolution, level of side lobes and output signal to noise ratio. This is illustrated in Figure16, which shows output signals for two different target speeds v.

For target speed v = 2 m/s the error in distance measurement ΔR is practically zero, the level of side lobes is equal –34 dB, and distance resolution is equal to 13 m. For target speed v = 10 m/s the error in distance measurement went up to ΔR = –10 m, the level of side lobes went up to –15 dB, and resolution to 24 m. Despite that, compared to the basic sonar result, which was ΔR = 155 m, the distance measurement error has been greatly improved.

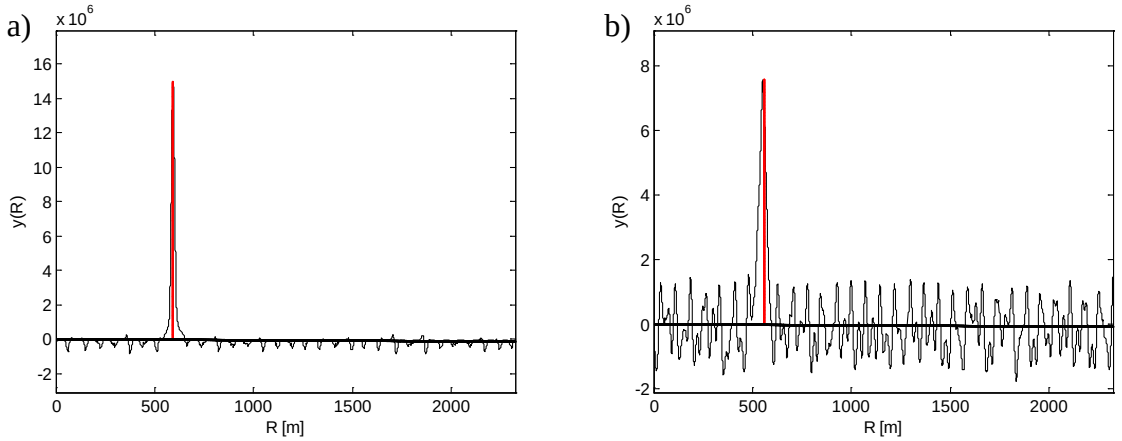

Fig. 16. The effect of speed on output signal: a) v = 2 m/s, b) v = 10 m/s.
(f_0 = 10 kHz, B = 2 kHz, B_e = 0.4 kHz, p = 0.2, N = 5, T_e = 0.1 s, p = 0.2).

Distance resolution depends primarily on the duration of the elementary signal T_e, and improves for shorter durations. It deteriorates, however, along with increases in target speed v and order of the sequence N.

Level of side lobes grows when time T_e is too short for a particular target speed v.

Output signal to noise ratio SNR_o is proportional to the input signal to noise ratio SNR_i, and depends on the other sonar parameters. It is a very complex relation, and cannot be discussed in detail within the framework of this article. This is why we are going to focus only on the most important relations.

The quality of sonar for particular detection conditions can be assessed by determining an improvement of SNR_o over SNR_i. The improvement is described with processing gain $PG = SNR_o/SNR_i$ [dB]. Let us denote the processing gain for a classical version of CW FM sonar as reference processing gain $PG_r = 10\log(B \cdot T)$. In the proposed solution processing gain cannot be greater than $PG = 10\log(B_e \cdot T_e)$, which makes it lower than PG_r by $10\log(B/B_e)$. In practice B/B_e = 2.5, hence the loss is 4 dB. The additional loss comes from a higher target speed v, and depends on the selection of the order of sequence N and the durations of elementary pulses and the averaging coefficient p. The effect of target speed v on output signal is illustrated in Figure 17. For target speed v = 2 m/s processing gain is PG = 31 dB, and for speed v = 5 m/s –PG =27 dB. For speed v = 0 processing gain increases to 33 dB and is lower by 5 dB than PG_r = 38 dB. For v = 0 the additional loss in gain amounts to 1 dB, for v = 2 m/s –3 dB, and for v = 5 m/s –7 dB. If processing gain is to be lower than in the basic sonar version, while maintaining detection conditions, emitted power has to increase, a cost that must be paid for a significant reduction in distance measurement error.

With a deteriorated output signal to noise ratio, the level of side lobes and distance resolution increase. In the situation shown in Figure 17, the level of side lobes went up from –16.6 dB to –10 dB, while resolution deteriorated from 7.5 m to 10.5 m. In both cases the distance measurement error did not change, and amounts to approx. 1 m.

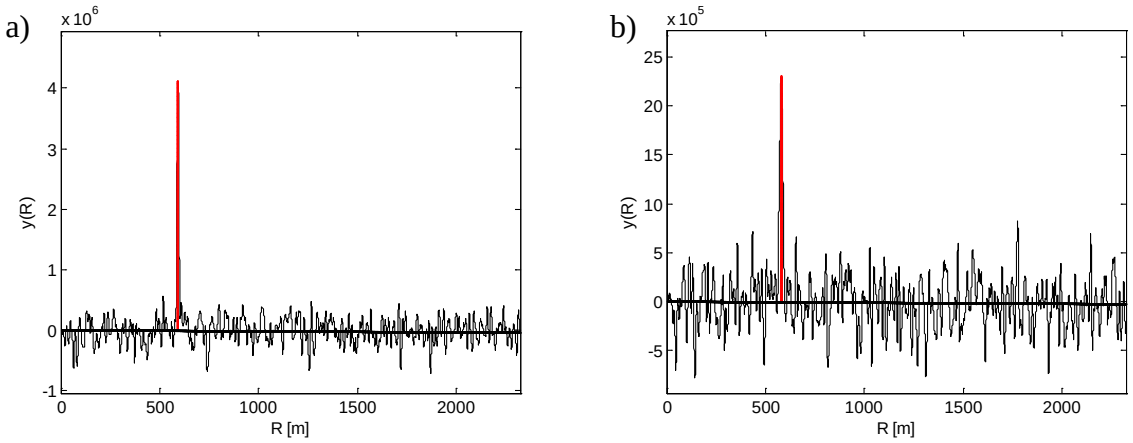

Fig. 17. The effect of target speed on output signal parameters for SNR_i = 0 dB:
a) v = 2 m/s, b) v = 5 m/s. (f_0 = 10 kHz, B = 2 kHz, B_e = 0.4 kHz, N = 5, T_e = 0.1 s, T_a = 10 ms).

5. Conclusion

There is a lot to suggest, based on our preliminary analysis, that the modified version of CW sonar offers a very promising solution. The use of a sounding signal which is a series made up of elementary HFM signals with opposite directions of modulation, switched by pseudorandom binary sequences, combined with a modified method of matched filtering on the receiving side, offers much more flexibility with parameter selection. The main advantage of the method is that it helps to achieve a radical reduction in distance measurement error involving a moving target, without limiting the range. There is only a slight deterioration in processing gain compared to the sonar with a single HFM signal. The objective of the next stages of the research is to conduct numerical simulations of the method, the use of other pseudo random sequences, and extend the scope of parameter changeability. The work will be aimed at achieving more accurate empirical relations, that can be translated into sonar design. Model tests in a test pool will be conducted. The results can then be compared to results from an earlier test using the basic version of CW FM silent sonar [5].

References

[1] S. A. Kramer, Doppler and acceleration tolerance of high-gain wide-band linear FM correlation sonar, Proc. IEEE, 33, 627-636, 1967.

[2] H. DeFerrari, J. Wylie, Ideal signals and processing for continuous active sonar, Acoustical Society of America, Proceedings of Meetings on Acoustics (ICA 2013 Montreal Canada), Vol. 19, 055058, 2013.

[3] S. J. Lourey, Frequency Hopping Waveforms for Continuous Active Sonar, Proceedings of 2015 IEEE International Conference on Acoustics, Speech, and Signal Processing, 1832 – 1835, Brisbane 2015.

[4] J. Marszal, R. Salamon, Detection Range of Intercept Sonar for CWFM Signals, Archives of Acoustics, Vol. 39, No 2. s. 215-230, 2014.

[5] J. Marszal, Experimental Investigation of Silent Sonar, Archives of Acoustics, Vol. 39, No 1, 103-115, 2014.

[6] J. Marszal, R. Salamon, Distance Measurement Errors in Silent FM-CW Sonar with Matched Filtering, Metrology and Measurement Systems, Vol. XIX, No. 2, 321-332, 2012.

[7] J. Marszal, R. Salamon, A. Jedel, Silent Sonar – State of the Art and Perspectives [in Polish], in Progress of Acoustics, editor K. J. Opieliński, Polish Acoustical Society, Wroclaw Division, 31-48, 2015.
[8] R. Salamon, J. Marszal, Estimating Intercept Range of Silent Sonar, in Hydroacoustics of Shallow Water edited by E. Kozaczka, G. Grelowska, Polish Academy of Sciences Institute of Fundamental Technological Research, 139-158, 2013.
[9] J. Marszal, R. Salamon, Silent Sonar for Maritime Security Applications, Acoustical Society of America, Proceedings of Meetings on Acoustics (ECUA 2012 Edinburgh UK), Vol. 17, 070082, 2013.
[10] J. Marszal, R. Salamon, L. Kilian, Application of Maximum Length Sequence in Silent Sonar, Hydroacoustics, Vol. 15, 143-152, 2012.
[11] J. Marszal, R. Salamon, K. Zachariasz, A. Schmidt, Doppler Effect in the CW FM Sonar, Hydroacoustics, Vol. 14, 157-164, 2011.
[12] J. Marszal, R. Salamon, A. Jedel, Sounding Signal, Emitted Especially by a Silent Sonar, and Demodulation Method for a Sounding Signal, Emitted Especially by a Silent Sonar [in Polish], Patent Pending No. P.407692, 2014.
[13] R. Salamon, J. Marszal, J. Schmidt, M. Rudnicki, Silent Sonar with Matched Filtration, Hydroacoustics, Vol. 14, 199-208, 2011.
[14] R. Salamon, J. Marszal, L. Kilian, A. Jedel, A. Raganowicz, Z. Ostrowski, Choice of the signals in silent sonar with matched filtration [in Polish], Open Seminar on Acoustics OSA'11, Vol. II, 257-266, 2011.
[15] R. van Vossen, S. P. Beerens, E. van der Spek, Anti-Submarine Warfare with Continuously Active Sonar, Sea Technology, Vol. 52**,** 11, 33-35, 2011.
[16] K. Wang, S. Chen, C. Liu , Y. Liu, Y. Xu, Doppler Estimation and Timing Synchronization of Underwater Acoustic Communication Based on Hyperbolic Frequency Modulation Signal, Proc. 2015 IEEE 12th International Conference on Networking, Sensing and Control, Howard Civil Service International House, Taipei, Taiwan, 75-80, 2015.
[17] L. Zurk, D. Rouseff , S. Schecklman, Exploitation of frequency information in Continuous Active Sonar, Proc. 22nd International Congress on Acoustics, Underwater Acoustics: ICA2016-446, Buenos Aires, 2016.